ARTICLES

Studies of Two-Photon Property of Intensely Luminescent Alkynyl−Phosphine Gold(I)−Copper(I) Complexes

Yi-Chih Lin,[†] Pi-Tai Chou,*[,†] Igor O. Koshevoy,[‡] and Tapani A. Pakkanen[‡]

Department of Chemistry, National Taiwan University, Taipei 106, Taiwan, R.O.C., and Department of Chemistry, University of Joensuu, Joensuu 80101, Finland

Received: May 1, 2009; Revised Manuscript Received: July 11, 2009

Two-photon absorption (TPA) spectra of a series of highly symmetric, strong phosphorescence Au^I-Cu^I complexes **1**−**7** bearing alkynyl−phosphine ligands in solution were obtained over the biological windows (760−840 nm) by the two-photon-induced emission technique under femtosecond laser excitation. The resulting TPA cross sections are further confirmed by the open-aperture Z-scan method, which offers the advantage of reducing the excited-state reabsorption for these long-lived phosphorescence dyes. The results of these two methods are mutually in good agreement, showing that complexes **1**−**7** exhibit moderately strong TPA cross section, for example, ∼710 GM at 760 nm for **1** in CH_2Cl_2. Owing to the highly centrosymmetric property, the resulting trend in TPA values for **1**−**7** can be rationalized by the unit of X-group−alkynyl−heterometallic-core−alkynyl−X-group fragment, categorized as A−π−D−π−A or D−π−A−π−D structural motif, which renders large changes in polarization upon excitation and provides significant near-IR TPA strength.

1. Introduction

Two-photon-absorbing materials have recently attracted significant interest because of their potential applications in 3D microfabrication,[1] photodynamic therapy,[2] two-photon imaging,[3–5] optical power limiting (OPL),[6] and optical data storage.[7] Although two-photon absorption (TPA) might generate the same photophysical processes as one-photon absorption (OPA) (high energy), two distinct advantages can be promptly pointed out: First, material will be protected from photodegradation by using lower-energy photons. Second, the quadratic dependence of TPA on intensity causes photophysics, photochemistry, or both to take place in a small focal region, allowing for more control in microfabrication and imaging applications. As for the design strategy, an ideal TPA material should possess chromophores that undergo large changes in polarization upon electronic excitation.[8] This criterion can be achieved through making structural motifs such as donor−π−acceptor (D−π−A), donor−π−acceptor−π−donor (D−π−A−π−D), or acceptor−π−donor−π−acceptor (A−π−D−π−A), and so on; many of such materials have been designed and synthesized and shown remarkable increases in TPA cross sections.[9] Among various approaches, d-block transition-metal complexes are thought to possess good nonlinear optical properties[10] because of their metal-to-ligand (MLCT) or ligand-to-metal (LMCT) charge-transfer bands per se, which are often associated with large optical nonlinearities in the UV−visible region. Moreover, coordinating a ligand containing highly polarizable π electrons to a metallic center could also yield electronic structures that possess weakly bound valence electrons, resulting in the enhancement of optical nonlinearities. In this regard, a prototypical example of conjugated organometallic molecules may be ascribed to the platinum(II) alkynyl complexes,[11] which generally have high linear transmission in the visible region, whereas the nonlinear absorption is significant over a wide spectral region, suited for OPL applications.

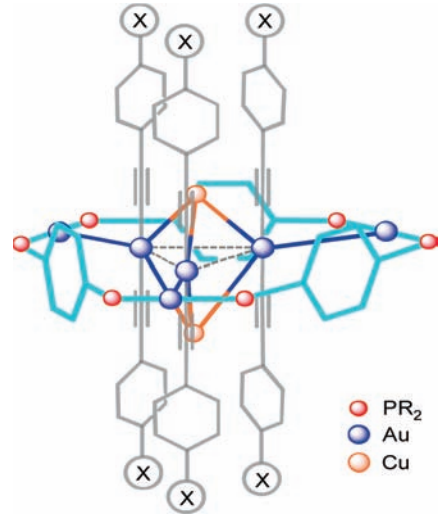

Figure 1. Schematic structure of dications $[\{Au_3Cu_2(C_2C_6H_4X)_6\}Au_3(PR_2C_6H_4PR_2)_3]^{2+}$ (**1**−**7**) (X = NO_2, H, OMe, NMe_2; R = Ph, NC_4H_4). (See Chart 1 for respective structure.)

Recently, we reported a new series of Au^I-Cu^I and Au^I-Ag^I heterometallic alkynyl−diphosphine (diphosphine = PPh_2-$(C_6H_4)_n$-PPh_2, n = 1, 2, 3) clusters,[12–16] which display a very intriguing structural pattern based on the heterometallic $[Au_xM_y(C_2Ph)_{2x}]^{y-x}$ fragments "wrapped" by the $[Au_3(diphosphine)_3]^{3+}$ "belts". (See Figure 1.) As a result,

* Corresponding author. E-mail: chop@ntu.edu.tw. Tel: +886-2-33663894. Fax: +886-2-23695208.
[†] National Taiwan University.
[‡] University of Joensuu.

10.1021/jp9040452 CCC: $40.75
Published on Web 07/27/2009

CHART 1: Structure of the Ligands and Related Complexes

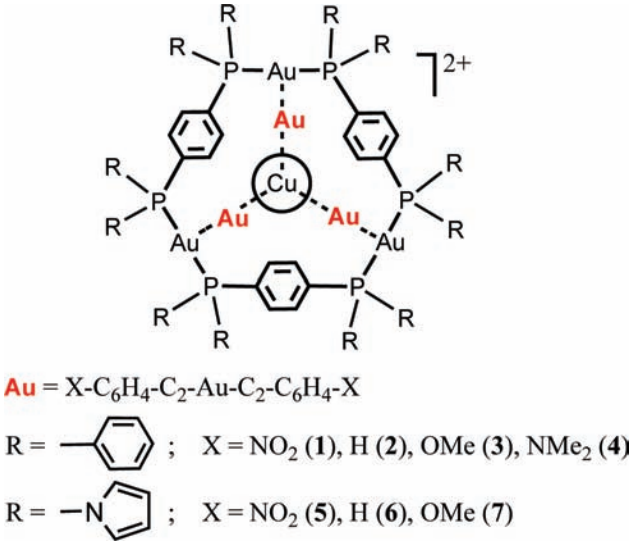

the lower-lying states of these complexes exhibit metal−ligand charge transfer properties, and intense phosphorescence was observed because of the heavy-metal-enhanced spin−orbit coupling. More importantly, owing to fully protected chromophore by bulky ancillary and bridging ligands, the phosphorescence is nearly inert to oxygen quenching. Note that except for those lanthanide complexes that have inner-shell atomic-like emission, the oxygen-quench-free phosphorescence is rarely reported and is unique among second- and third-row transition-metal complexes.

The above properties led us to examine the applicability of these heterometallic alkynyl−diphosphine clusters to time-resolved phosphorescence imaging. Of particular interest is the two-photon-induced phosphorescence property latently suited for 3D imaging. In a preliminary work, we primitively measured the TPA value of a heterometallic complex, $[\{Au_8Ag_{10}(C_2Ph)_{16}\}\{(PhC_2Au)_2PPh_2(C_6H_4)_3PPh_2\}_2]^{2+}$. The resulting TPA cross section of 104.9 GM (800 nm)[16] encourages us to perform extensive studies on the nonlinear properties of relevant Au^I-Cu^I or Au^I-Ag^I alkynyl−diphosphine clusters. An ideal compound suited for time-resolved imaging requires the fulfillment of the following criteria: (i) The phosphoresce is intense with a decent lifetime of, for example, several microseconds. (ii) The phosphorescence is subject to minor-to-negligible oxygen quenching in aerated solutions. (iii) These complexes should offer a good TPA cross section in the biological windows.

Herein, we report the comprehensive studies of TPA properties for a series of highly symmetric Au^I-Cu^I complexes depicted in Chart 1. Owing to the highly centrosymmetric property, we expect that the trend in TPA values, if measurable, may be rationalized by the classification of X-group−alkynyl−heterometallic-core−alkynyl−X-group fragment into A−π−D−π−A and D−π−A−π−D structural motif (vide infra). In this study, the TPA cross sections were measured using the two-photon-induced emission (TPIE) technique together with direct TPA cross-section measurement via open-aperture Z-scan method. The latter method, being with 1 kHz femtosecond laser excitation, is able to reduce the excited-state reabsorption and hence minimize the artifact. Detailed experimental setup, analyses, and discussion are elaborated in the following sections.

2. Experimental Section

2.1. Materials. Compounds **1**−**7** were prepared similarly to the previously reported procedure.[15] The clusters obtained were repetitiously recrystallized, and their purity was confirmed by the ^1H and ^{31}P NMR spectra. The synthetic and characterization details are given in the corresponding section of the Supporting Information.

2.2. Steady-State Measurements. The linear absorption and emission spectra were recorded on a Hitachi (U-3310) spectrophotometer and an Edinburgh (FS920) fluorometer, respectively. Both wavelength-dependent excitation and emission response of the fluorometer have been calibrated. Coumarin 480 in methanol, with quantum yield of ~0.87, served as the standard for measuring the quantum yield. The error of the quantum yield measurement was in the range of <2% (three replica). Lifetime studies were performed with an Edinburgh FL 900 photon-counting system using a hydrogen-filled lamp as the excitation source. Data were analyzed using the nonlinear least-squares procedure in combination with an iterative convolution method. The emission decays were analyzed by the sum of exponential functions, which allows partial removal of the instrument time broadening and consequently renders a temporal resolution of ~300 ps.

2.3. Two-Photon Induced Emission Method. The setup for TPIE measurement is depicted in Scheme 1 and is similar to that used by Xu et al.[17] In brief, a femtosecond-mode-locked Ti/sapphire laser (Spectra Physics) generates 120 fs pulses at a repetition rate of 82 MHz with an average power of 1.4 W. The laser beam was attenuated to optimum power and focused on a sample cell (1 cm) by a lens with a focal length of 6 cm. To minimize the effects of reabsorption, the excitation beam was focused as close as possible to the edge of the quartz cell, which faced the slit of the imaging spectrograph. The TPIE was detected in a direction perpendicular to the pump beam. The emission was then focused by a lens with the focal length 8 cm into an optical spectrum analyzer. The optical spectrum analyzer consists of a CCD with a detector controller (PI-MAX camera, Princeton Instruments Inc.) in conjunction with a high-throughput monochromator (SP2300i, Acton Reaearch Corporation).

TPA and two-photon emission (TPE) cross sections (σ_{TPA} and σ_{TPE}, respectively) are basic parameters for evaluating a material's TPA and two-photon-excited emission properties. From the two-photon-excited emission intensity data, σ_{TPA} and σ_{TPE} can be evaluated using eqs 1 and 2 expressed below[18]

$$\sigma_{TPE} = \sigma_{TPE,r}\frac{Fn_rC_r}{F_rnC} \quad (1)$$

$$\sigma_{TPA} \times \Phi = \sigma_{TPE} \quad (2)$$

where r stands for the reference compound, n denotes the refractive index of the solvent, F represents the integrated emission intensity, and C is the concentration of the molecules in solution. The TPE cross section, σ_{TPE}, is supposed to be linearly dependent on the TPA cross section (σ_{TPA}) with the two-photon-excited emission quantum yield Φ' as the coefficient. In most reports, the one-photon-excited emission quantum yield Φ was adopted instead of Φ' because of the difficulty in measuring Φ'. By referencing the TPE cross section of Coumarin 480 to be 146.2 GM (1 GM = 10^{-50} cm^4·s photon^{-1}).[19] The two-photon-excited emission of Coumarin 480 was measured as a standard under the same experimental

SCHEME 1: Experimental Setup for (A) TPIE and (B) Open-Aperture Z-Scan Technique[a]

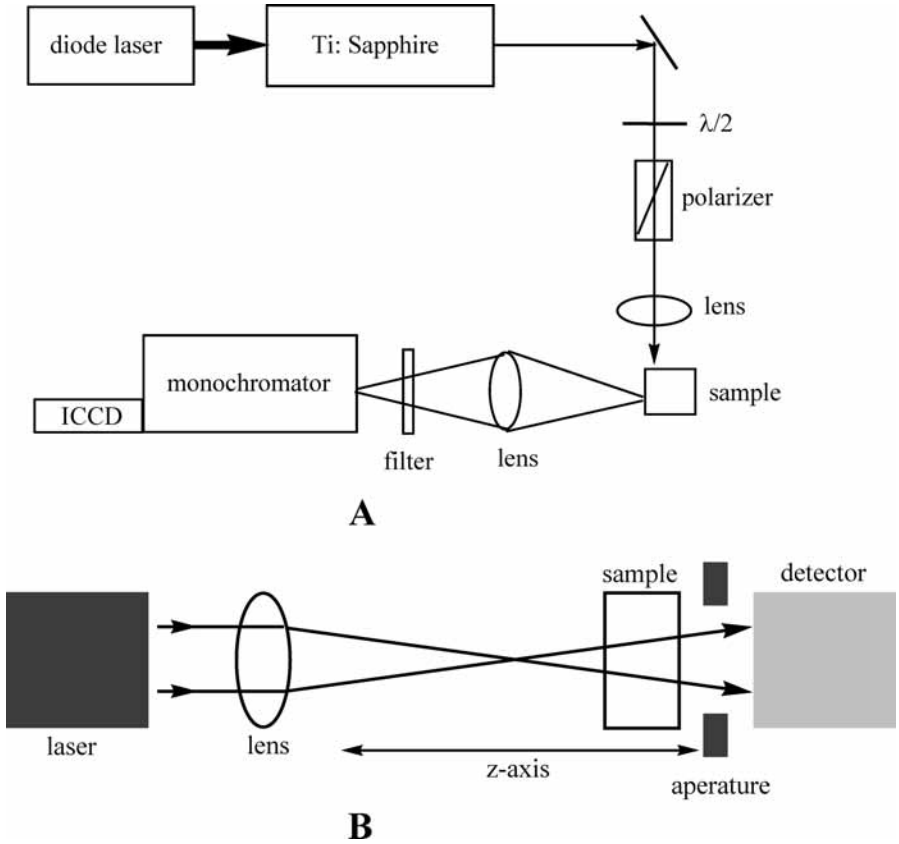

[a] ICCD: intensified charge coupled detector. λ/2: half-wave plate.

conditions. We obtained the relative TPE cross sections of the titled compounds by comparing their two-photon-excited emission to that of Coumarin 480 under exactly the same experimental conditions. The quadratic dependence of the emission intensity on excitation power was checked for all excitation wavelengths, indicating a pure TPA process and negligible influence of saturation and photobleaching effects. The concentrations of compounds **1**−**7** for the comparative two-photon emission measurements are consistent with the quantum yield determination to be 1×10^{-5} M in dichloromethane. The error of TPA measurement was in the range of <10% (four replica).

2.4. Open Aperture Z-Scan Method. We conducted the open aperture Z-scan experiments by using essentially the same experimental setup and procedure as that previously described.[20] A brief sketch of the setup is depicted in Scheme 1B. In this study, a mode-locked Ti/sapphire laser (Tsunami, Spectra Physics) produced a single Gaussian pulse that was coupled to a regenerative amplifier that generated a ∼200 fs, 1 mJ pulse (760−840 nm, 1 kHz, Spitfire Pro, Spectra Physics). The pulse energies, after suitable attenuation, were reduced to 0.3 to 0.65 μJ. After passing through an $f = 30$ cm lens, the laser beam was focused and passed through a 2.00 mm cell filled with the sample solution (concentrations in the range of 5×10^{-4} to 2.5×10^{-3} M), and the beam radius at the focal position is 3.82×10^{-3} cm.

When the sample cell changed its position along the beam direction (z axis), the transmitted laser beam from the sample cell was detected by a photodiode (PD-10, Ophir). The model used to fit the Z-scan data assumes a coherent TPA process and was already thoroughly discussed in ref 19. Accordingly, in theory, the TPA-induced decrease in transmittance, $T(z)$, can be expressed as eqs 3 and 4, and TPA coefficient (β) can be obtained from experimental data by fitting Z-scan curves to relationships 3 and 4

$$T(z) = \sum_{n=0}^{\infty} \frac{(-q)^n}{(n+1)^{3/2}} \tag{3}$$

$$q = \frac{\beta I_0 L}{1 + \frac{z^2}{z_0^2}} \tag{4}$$

where n is an integer number from 0 to ∞ and has been truncated at $n = 1000$, L is the sample length, I_0 is the input intensity, z is the sample position with respect to the focal plane, and z_0 is the diffraction length of the incident beam (Rayleigh range). After obtaining the TPA coefficient (β), TPA cross section (σ_{TPA}) can be deduced by using eq 5

$$\beta = \frac{\sigma_{TPA} N_A d \times 10^{-3}}{h\nu} \tag{5}$$

where N_A is Avogadro's number, d is the concentration, h is Planck's constant, and υ is the frequency of the incident beam. As for the open aperture Z-scan experiments, we have measured TPA cross sections of a well-known TPA dye, coumarin 480, to ensure that the TPA cross-section values were not overestimated. (See Figure S2 of the Supporting Information). The resulting value of 165.1 GM is consistent with the reported data of 168.2 GM within 5% uncertainty (five replicas).

TABLE 1: Summary of OPA and TPA Properties

	λ_{ab}/nm (10^{-3} ε/cm^{-1}M^{-1})	λ_{em}/nm	Φ^a	Φ^b	$\tau_{obsd}/\mu s^{a,c}$	σ_{TPA}/GM^{d,e}	σ_{TPA}/GM^{d,f}	σ_{TPE}/GM^{a,d,e}
1	265 (77.2), 351 (44.8), 408sh (28.3)	576	0.73	0.93	3.15	346.3 ± 35	386.7 ± 20	252.8
2	263 (80.7), 336sh (21.1), 403 (26.0)	594	0.67	0.96	3.69	169.5 ± 17	191.6 ± 10	113.5
3	264 (79.6), 287sh (54.0), 402 (20.8)	620	0.33	0.77	2.60	135.3 ± 14	153.6 ± 8	44.7
4	264 (70.8), 294 (58.8), 395 (32.5)	686	0.04	0.10	0.31	238.5 ± 24	245.3 ± 13	9.5
5	333 (54.4)	607	0.55	0.62	4.81	183.8 ± 19	215.5 ± 11	101.1
6	253 (72.8), 401 (18.3)	650	0.26	0.61	3.72	145.6 ± 15	171.4 ± 9	37.8
7	260 (74.1), 398 (20.7)	671	0.12	0.19	1.61	112.0 ± 11	130.7 ± 7	13.4

[a] Measured in aerated CH_2Cl_2 solutions, and Coumarin 480 in methanol was used as a standard for the quantum yield (Φ) measurements. [b] Measured in degassed CH_2Cl_2 solutions, and Coumarin 480 in methanol was used as a standard for the quantum yield (Φ) measurements. [c] λ_{excit} = 450 nm and monitored the emission at peak maximum. [d] TPA cross-section (σ_{TPA}) measured at 800 nm. [e] Samples in aerated dichloromethane and the reference dye, coumarin 480, in methanol were all prepared at a concentration of 1×10^{-5} M. [f] Measured by open-aperture Z-scan method in aerated dichloromethane.

3. Results and Discussion

Complexes **1**−**7** adopt a similar molecular framework, namely, an assembly of heterometallic alkynyl clusters $[Au_3Cu_2(C_2C_6H_4X)^6]^-$ and cationic $[Au_3(PR_2C_6H_4PR_2)_3]^{3+}$ (Figure 1), the structures of which have been well characterized by NMR spectroscopy and ESI-MS measurements.[15] All complexes exhibit highly intense emission in the region of 500−800 nm. In degassed CH_2Cl_2, the quantum yield (Φ) of emission was measured to be >0.1 (e.g., $\Phi \approx 0.93$ for **1**, Table 1). This, together with the observed lifetime of >0.3 μs (Table 1), renders radiative lifetime (τ_r) of several microseconds for **1**−**7** ($\tau_r \approx 9.6$ μs for **4**). The results unambiguously warrant the emission originating from spin-forbidden phosphorescence. The results also unveil a good correlation between the molecular structure (Figure 1) and photophysical data, such as emission energy gap, listed in Table 1. For complexes **1**−**7**, the emission peak wavelength reveals bathochromic shift as the electron-donating (accepting) ability of the alkynyl (diphosphines) ligands increases. Such a tendency implies that the lowest-lying transition in the triplet manifold should incorporate alkynyl ligands (diphosphines) as HOMO (LUMO), which is consistent with the previous assignment based on frontier orbital analyses.[15] Note that a remarkable feature of the phosphorescence property for the titled complexes lies in its low O_2 quenching effect. For example, the phosphorescence quantum yield of complex **1** still remains ~80% ($\Phi_p \approx 0.73$, Table 1) upon aeration, which has been rationalized by the fact that the core phosphorescent chromophores are well-protected by the unique framework consisting of bulky ancillary and bridging ligands. For further confirmation of this viewpoint, we then measured the phosphorescence lifetime as a function of the power of laser excitation (375 nm diode laser, PicoQuant, model PDL-800-D, 50 ps duration time). In theory, increasing the excitation intensity should render more triplet state (T_1) population, which should enhance triplet−triplet annihilation, resulting in the quench of phosphorescence. As shown in Figure S3 of the Supporting Information, the phosphorescence lifetime of compound **1** upon high-power excitation (50 pJ/pulse) versus low-power excitation (pulse energy is 5 pJ) in degassed CH_2Cl_2, within experimental error, is essentially the same (4.80 μs).[15] The results clearly reveal that the phosphorescence of **1** is inert to both O_2 quenching and triplet−triplet annihilation, supporting the aforementioned proposal of ligands protection on the emitting chromophore. For convenience and practical concern, hereafter the results and discussion of OPA and TPA properties are mainly based on the aerated solution unless otherwise specified.

Figure 2 shows the normalized TPIE spectra of **1**−**7** in CH_2Cl_2. Clearly, the TPIE, in terms of spectral feature and peak wavelength, is identical to that of the one-photon excitation

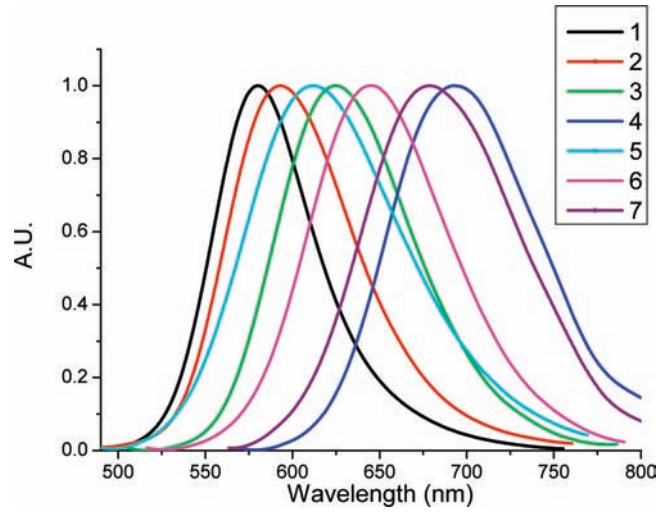

Figure 2. Normalized two-photon-induced emission spectra of **1**−**7** in aerated dichloromethane at room temperature. The excitation wavelength is at 840 nm for all emissions acquired.

emission (Supporting Information), confirming its origin from the phosphorescence. Using complex **1** as an example, as depicted in the inset of Figure 3, the up-converted phosphorescence intensity is linearly dependent on the square of the incident laser power, firmly supporting the occurrence of TPA. The TPA spectra of compounds **1**−**7** in CH_2Cl_2, measured by TPIE method, are displayed in Figure 3, which clearly show a good σ_{TPA} value in the range of 760−840 nm, reaching a value of >200 GM at 760 nm for all titled compounds. Because the reported value is an average of four measurements using different batches and the standard deviation is <10%, the result is considered to be reproducible. Even at 800 nm, a wavelength that is practically useful for biological applications, these compounds still exhibit appreciably large σ_{TPA} values ranged from 130 GM to 390 GM.

One salient feature of the TPA spectra is the resolution of a TPA peak in the region of 790−810 nm (Figure 3B), which is nearly coincident with the OPA peak (Figure 3A) for these complexes. This seemly violation of selection rule may qualitatively be rationalized by a different coupling of the electronic transition to nontotally symmetric vibrations in respective OPA and TPA.[11] Furthermore, an increase in the TPA cross sections at <780 nm is observed for all complexes. Conversely, OPA shows a relatively lower absorptivity around 380−390 nm. Therefore, the TPA spectra in this region can be assigned to a one-photon-forbidden, two-photon-allowed, gerade−gerade transition. This, in turn, implies that the absorbing species possesses inversion symmetry and hence the heterometallic core of the complexes should be incorporated into the TPA chromophore.

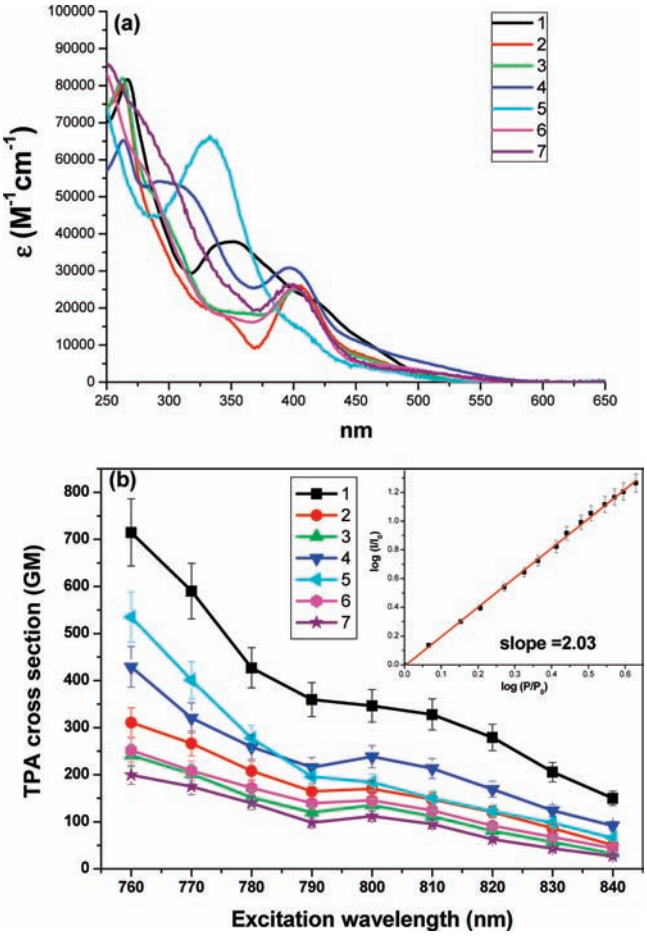

Figure 3. (a) One-photon absorption spectra of **1**−**7** in CH_2Cl_2 at room temperature. (b) Two-photon excitation spectrum (760−840 nm) of compound **1**−**7** in dichloromethane. Insert: The log−log plot of normalized excitation power (P/P_0) versus normalized two-photon emission intensity (I/I_0) of compound **1**.

In a complementary approach, we then performed the open aperture Z-scan experiments to examine the reliability of σ_{TPA} values obtained from TPIE measurements. Figure 4 shows a typical Z-scan and fitting curves of the titled compounds in CH_2Cl_2. For all compounds studied, the experimental data points and the corresponding fitting curve show high degrees of correlation. The TPA cross sections of **1**−**7**, measured by open-aperture Z-scan method, are then calculated to be 386.7 GM, 191.6 GM, 153.6 GM, 245.3 GM, 215.5 GM, 171.4 GM, and 130.7 GM, respectively, at 800 nm. (See Table 1.) Obviously, the results obtained by Z-scan method are relatively larger than that of the TPIE measurement by 5−20%. For complexes **1**−**7**, mainly because of the 82 MHz femtosecond laser excitation in the TPIE measurement, the long-lived triplet state (several microseconds) may lead to the excited state reabsorption. We thus reasonably treat the TPA cross section measured by TPIE technique as a lower-limit. Nevertheless, as listed in Table 1, both methods render the same trend of the TPA cross sections.

Prior to data analyses, a simplified TPA theory suited to the above titled complexes is briefly described here. Because of the complicated two-photon allowed transitions (gerade−gerade transition), which are involved in the frontier orbitals of heterometallic core, bridging ligand, and X-substituting alkynes, it is not easy to determine clearly the relationship between TPA cross section and electron-withdrawing ability at the X position by theoretical calculation. If the molecule is centrosymmetric, then the value of σ_{TPA} for a transition from ground state, g, to a final state, f, at the maximum of a TPA band with a Lorentzian line shape is given by eq 6[21]

$$\sigma_{TPA}^{max} \approx C\frac{\mu_{gi}^2\mu_{if}^2}{[(E_{gi}/h\nu) - 1)]^2\Gamma_f} \quad (6)$$

where μ_{nm} is the amplitude of the oscillating (transition) dipole moment (or polarization) induced by electronic field of a light wave whose frequency matches the energy difference between states m and n, E_{gi} is the energy gap between the ground state and an intermediate state, i, $h\nu$ is the photon energy, C is a constant, depending on relative orientation of (transition) dipole moments μ_{gi} and μ_{if}, and Γ_f is the line width of state f. Donor and acceptor groups at the center and the ends of the molecule can enhance the dipole moments, μ_{gi} and μ_{if}.

The symmetrical structure geometry (D_{3h} symmetry group), shown in Figure 1, is believed to account for the origin of the TPA property for the titled complexes. It has been well known that one- and two-photon absorptions adhere to different selection rules in a centrosymmetric molecule. For the molecule possessing central symmetry, a change in the parity between the initial and final states (wave functions) is required for every photon involved in the electric dipole transitions. Changes of parity are required for a one-photon transition, whereas two-photon transitions must have initial and final states both possessing the same parity; that is, it requires the symmetrical structure geometry. From the structure point of view, the X-substituent−alkynyl−heterometallic-core−alkynyl−X-substituent fragments of the titled complexes can be classified into A−π−D−π−A, D−π−A−π−D, D_2−π−D_1−π−D_2, or A_2−π−A_1−π−A_2 structural motif that is subject to large changes in polarization upon excitation and offers significant TPA cross section in the near-IR region.[9] For OPA, using complex **1** as a model, the 400 nm absorption peak of **1** (and **2**−**7** as well) is mainly due to the transition of Cu−π−alkynyl fragment in combination with the metal- and cluster-centered transitions, which can be partially described as a metal-to-ligand charge-transfer (MLCT) transition.[12,22] Combining MLCT transition and the terminal electron-acceptor (−NO_2), it is reasonable to classify compound **1** into an A−π−D−π−A structural motif in which the X substituent (−NO_2) represents the electron acceptor (A) and the phenyl alkynes fragment denotes the conjugated bridge (π), whereas the composition of heterometallic core and bridging ligand forms the electron donator part (D). In fact, complexes **1**−**4** possess the same bridging ligand, $PPh_2C_6H_4PPh_2$, whereas the difference lies in the variation of the X-substituting group at the para position, as marked in Figure 1.

As implicitly expressed in eq 6, for the A−π−D−π−A system, a key factor to increase TPA cross section lies in the increase in the electron-withdrawing ability of the X substituent. Accordingly, the TPA cross sections decrease with a trend of **1** (346.3 GM) > **2** (169.5 GM) > **3** (135.3 GM), which correlates well with the decrease in the strongly electron-accepting strength of the X substituent in the order of −NO_2 (**1**) > −H (**2**) > −OMe (**3**). However, compound **4** does not follow the descent trend based on the A−π−D−π−A structural motif. Owing to the strong electron-donating ability of X = −NMe_2 in **4**, the results led us to propose a switch of structural motif to either D_2−π−D_1−π−D_2 or D−π−A−π−D. Realizing that **3** and **4** possess the same class of electron-donating group, that is, −OMe and −NMe_2, respectively, this viewpoint is firmly supportive by the steep increase in the TPA cross sections from

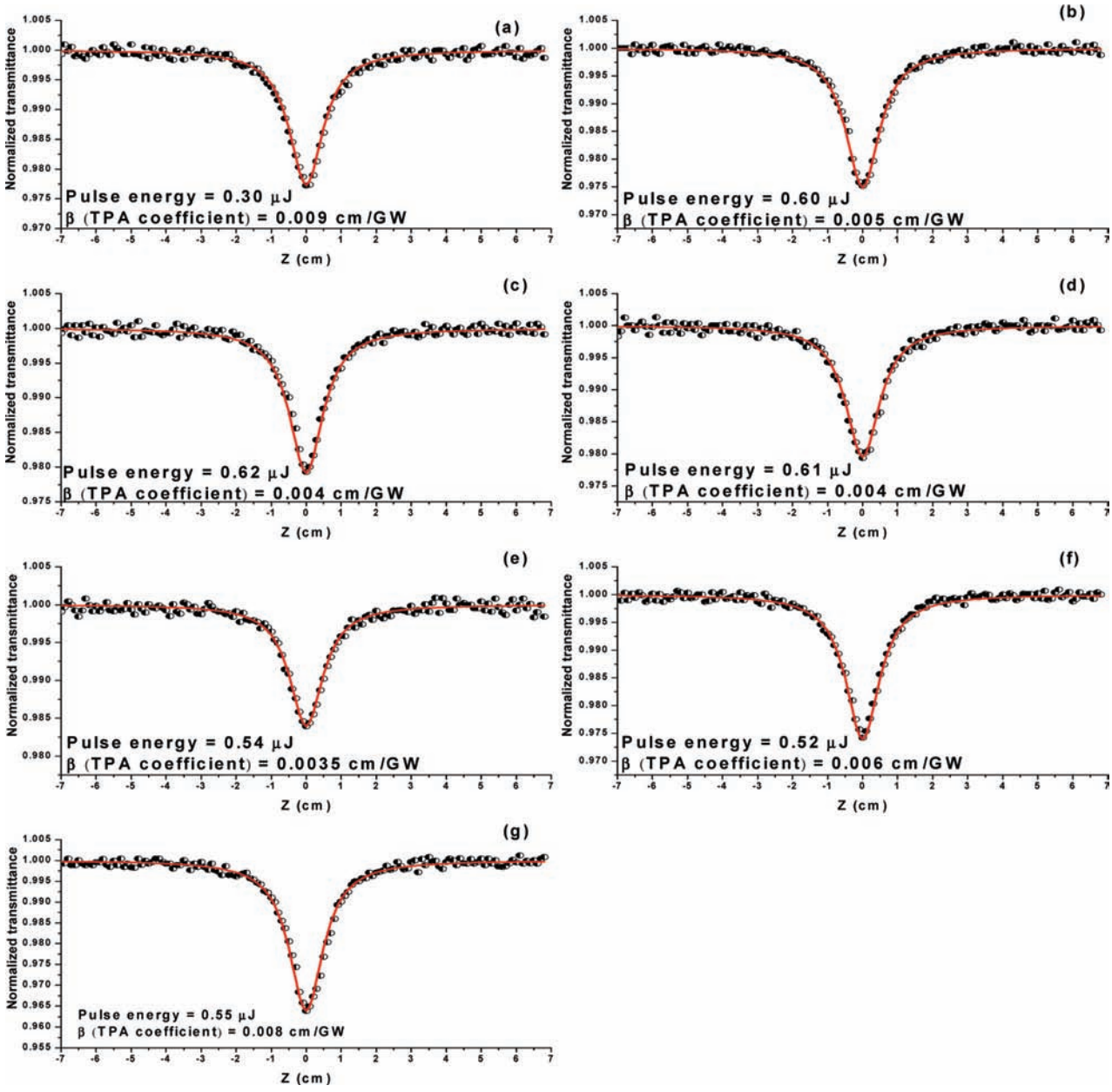

Figure 4. Z-scan experimental data of (a) compound **1** in dichloromethane (9.6×10^{-4} M) (circles), (b) compound **2** in dichloromethane (1.1×10^{-3} M) (circles), (c) compound **3** in dichloromethane (1.1×10^{-3} M) (circles), (d) compound **4** in dichloromethane (6.7×10^{-4} M) (circles), (e) compound **5** in dichloromethane (6.7×10^{-4} M) (circles), (f) compound **6** in dichloromethane (1.4×10^{-3} M) (circles), and (g) compound **7** in dichloromethane (2.5×10^{-3} M) (circles) in a 2 mm cell. Solid lines are the result of a fit to the data points.

135.3 GM in **3** to 238.5 GM in **4.** On the basis of eq 6, the result also implies a large change of (transition) dipole moment from **3** to **4** in terms of magnitude and orientation. Therefore, it is reasonable to ascribe the structural motifs of D−π−A−π−D for **4**, in which the heterometallic core is reversely treated as an accepting site, to account for the TPA results.

As for complexes **5**−**7**, except for the bridging ligand, PR_2-$C_6H_4PR_2$ (R = NC_4H_4), they all possess similar A−π−D−π−A structural motif with respect to **1**−**3**, and the resulting TPA in the order of **5** (183.8 GM) > **6** (145.6 GM) > **7** (112.0 GM) can be well rationalized by the decrease in the electron-accepting strength of the X substituent of $-NO_2$ (**5**) > −H (**6**) > −OMe (**7**). It is also noteworthy that the TPE cross sections (σ_{TPE}), defined by the product of the TPA cross section and emission quantum yield, can be regarded to be a consequence of both enhancement of TPA cross section and quantum yield. The σ_{TPE} values of compound **1**−**4** are 252.8 GM, 113.5 GM, 44.7 GM, and 9.5 GM, respectively, as listed in Table 1. Importantly, the enhancement of TPA cross section and quantum yield reflect the strength of the terminal acceptor ($-NO_2$ > −H > −OMe > $-NMe_2$) and exhibit an increase in the σ_{TPE} value, up to, for example, 27-fold, between compounds **1** and **4**. Another class of complexes, **5**−**7**, also shows similar enhancement (approximately seven-fold). Note that the large TPE cross section provides high contrast and resolution in both two-photon laser scanning imaging and time-resolved two-photon emission imaging.[4,5]

4. Conclusions

The highly symmetric Au^I−Cu^I alkynyl complexes are found to show TPA and two-photon-induced luminescence properties. The substituents of these complexes could be readily modified with electron-donating or electron-withdrawing substituents,

which provide a large TPA cross section in biological windows (760 to 840 nm). The results can be well explained by the structural motif of the titled complexes **1**−**7** being classified into A−π−D−π−A (**1**−**3**, **5**−**7**) and D−π−A−π−D (**4**) motifs to account for the TPA properties. For A−π−D−π−A configuration, TPA cross sections decrease as the electron-withdrawing strength of the X substituent decreases. For complex **4**, the strong electron-donating group (−NMe_2) switches the corresponding structural motif to D−π−A−π−D configuration, resulting in a significant increase in TPA value (cf. **3**). The intense phosphorescence, very minor O_2 quenching, and moderately strong TPA property demonstrated here warrant promising potential for alkynyl−phosphine Au(I)−Cu(I) complexes in two-photon emission imaging as well as phosphorescence dyes in time-resolved imaging.[4–6]

Acknowledgment. We thank the National Science Council (grant nos. 99-1989-2004) and the Academy of Finland (I.O.K.) for financial support.

Supporting Information Available: Synthesis section of the titled complexes. This material is available free of charge via the Internet at http://pubs.acs.org.

References and Notes

(1) (a) Zhou, W.; Kuebler, S. M.; Braun, K. L.; Yu, T.; Cammack, J. K.; Ober, C. K.; Perry, J. W.; Marder, S. R. *Science* **2002**, *296*, 1106. (b) Kawata, S.; Sun, H.-B.; Tanaka, T.; Takada, K. *Nature* **2001**, *412*, 697. (c) Sun, H.-B.; Mizeikis, V.; Xu, Y.; Juodkazis, S.; Ye, J.-Y.; Matsuo, S.; Misawa, H. *Appl. Phys. Lett.* **2001**, *79*, 1. (d) Maruo, S.; Nakamura, O.; Kawata, S. *Opt. Lett.* **1997**, *22*, 132.

(2) Denk, W.; Strickler, J. H.; Webb, W. W. *Science* **1990**, *248*, 73.

(3) (a) Bhawalkar, J. D.; Kumar, N. D.; Zhao, C. F.; Prasad, P. N. *J. Clin. Laser Med. Surg.* **1997**, *15*, 201. (b) He, G. S.; Markowicz, P. P.; Line, P.-C.; Prasad, P. N. *Nature* **1999**, *415*, 767. (c) Xu, C.; Zipfel, W.; Shear, J. B.; Williams, R. M.; Webb, W. W. *Proc Natl. Acad. Sci. U.S.A* **1996**, *93*, 10763. (d) Larson, D. R.; Zipfel, W. R.; Williams, R. M.; Clark, S. W.; Bruchez, M. P.; Wise, F. W.; Webb, W. W. *Science* **2003**, *300*, 1434.

(4) Kölër, R. H.; Cao, J.; Zipfel, W. R.; Webb, W. W.; Hanson, M. R. *Science.* **1997**, *276*, 2039.

(5) Botchway, S. W.; Charnley, M.; Haycock, J. W.; Parker, A. W.; Rochester, D. L.; Weinstein, J. A.; Williams, J. A. G. *Proc. Natl. Acad. Sci. U.S.A.* **2008**, *105*, 16071–16076.

(6) (a) He, G. S.; Xu, G. C.; Prasad, P. N.; Reinhardt, B. A.; Bhatt, J. C.; McKellar, R.; Dillard, A. G. *Opt. Lett.* **1995**, *20*, 435. (b) Calvete, M.; Yang, G. Y.; Hanack, M. *Synth. Met.* **2004**, *141*, 231.

(7) (a) Parthenopoulos, D. A.; Rentzepis, P. M. *Science* **1989**, *245*, 843. (b) Strickler, J. H.; Webb, W. W. *Opt. Lett.* **1991**, *16*, 1780. (c) Belfield, K. D.; Schafer, K. J. *Chem. Mater.* **2002**, *14*, 3656.

(8) Marder, S. R.; Gorman, C. B.; Meyers, F.; Perry, J.; Bourhill, G.; Bredas, J.-L.; Pierce, B. M. *Science* **1994**, *265*, 632.

(9) (a) Prasad, P. N.; Reinhardt, B. A. *Chem. Mater.* **1990**, *2*, 660. (b) Larson, E. J.; Friesen, L. A.; Johnson, C. K. *Chem. Phys. Lett.* **1997**, *265*, 161. (c) Albota, M.; Beljonee, D.; Bredas, J.-L.; Ehrlich, J. E.; Fu, J.-Y.; Heikal, A. A.; Hess, S. E.; Kogej, T.; Levin, M. D.; Marder, S. R.; McCord-Maughon, D.; Perry, J.; Rockel, H.; Rumi, M.; Subramanian, G.; Webb, W. W.; Wu, X. L.; Xu, C. *Science* **1998**, *281*, 1653. (d) Chung, S. J.; Kim, K. S.; Lin, T. C.; He, G. S.; Swiatkiewicz, J.; Prasad, P. N. *J. Phys. Chem. B* **1999**, *103*, 10741. (e) Oberle, J.; Bramerie, L.; Jonusauskas, G.; Rullier, C. *Opt. Commun.* **1999**, *169*, 325. (f) Belfield, K. D.; Hagan, D. J.; Van Stryland, E. W.; Schafer, K. J.; Negres, R. A. *Org. Lett.* **1999**, *1*, 1575. (g) Kannan, R.; He, G. S.; Yuan, L.; Xu, F.; Prasad, P. N.; Dombroskie, A. G.; Reinhardt, B. A.; Baur, J. W.; Vaia, R. A.; Tan, L. S. *Chem. Mater.* **2001**, *13*, 1896. (h) Mongrin, O.; Porres, L.; Katan, C.; Pons, T.; Mertz, J.; Blanchard-Desce, M. *Tetrahedron Lett.* **2003**, *44*, 8121. (i) Brousmiche, D. W.; Serin, J. M.; Frechet, J. M. J.; He, G. S.; Lin, T. C.; Chung, S. J.; Prasad, P. N. *J. Am. Chem. Soc.* **2003**, *125*, 1448. (j) Marder, S. R. *Chem. Commun.* **2006**, 131.

(10) (a) McKay, T. J.; Bolger, J. A.; Staromlynska, J.; Davy, J. R. *J. Chem. Phys.* **1998**, *108*, 5537. (b) McKay, T. J.; Staromlynska, J.; Davy, J. R.; Bolger, J. A. *J. Opt. Soc. Am. B* **2001**, *18*, 358. (c) McKay, T. J.; Staromlynska, J.; Wilson, P.; Davy, J. R. *Appl. Phys.* **1999**, *85*, 1337. (d) Staromlynska, J.; Chapple, P. B.; Davy, J. R.; McKay, T. J. *Proc. SPIE* **1994**, *2229*, 59. (e) Staromlynska, J.; McKay, T. J.; Bolger, J. A.; Davy, J. R. *J. Opt. Soc. Am. B* **1998**, *15*, 1731. (f) Staromlynska, J.; McKay, T. J.; Wilson, P. *J. Appl. Phys.* **2000**, *88*, 1726. (g) Vestberg, R.; Malmstrøm, E.; Eriksson, A.; Lopes, C.; Lindgren, M. *Proc. SPIE* **2004**, *5621*, 31.

(11) (a) Rogers, J. E.; Slagle, J. E.; Krein, D. M.; Burke, A. R.; Hall, B. C.; Fratini, A.; McLean, D. G.; Fleitz, P. A.; Cooper, T. M.; Drobizhev, M.; Makarov, N. S.; Rebane, A.; Kim, K.-Y.; Farley, R.; Schanze, K. S. *Inorg. Chem.* **2007**, *46*, 6483. (b) Yang, Z. D.; Feng, J. K.; Ren, A. M. *Inorg. Chem.* **2008**, *47*, 10841. (c) Tao, C. H.; Yang, H.; Zhu, N. Y.; Yam, V. W. W.; Xu, S. J. *Organometallics* **2008**, *27*, 5453.

(12) Koshevoy, I. O.; Koskinen, L.; Haukka, M.; Tunik, S. P.; Serdobintsev, P. Y.; Melnikov, A. S.; Pakkanen, T. A. *Angew. Chem., Int. Ed.* **2008**, *47*, 3942.

(13) Koshevoy, I. O.; Karttunen, A. J.; Tunik, S. P.; Haukka, M.; Selivanov, S. I.; Melnikov, A. S.; Serdobintsev, P. Y.; Khodorkovskiy, M. A.; Pakkanen, T. A. *Inorg. Chem.* **2008**, *47*, 9478.

(14) Koshevoy, I. O.; Karttunen, A. J.; Tunik, S. P.; Haukka, M.; Selivanov, S. I.; Melnikov, A. S.; Serdobintsev, P. Y.; Pakkanen, T. A. *Organometallics* **2009**, *28*, 1369.

(15) Koshevoy, I. O.; Lin, Y. C.; Karttunen, A. J.; Chou, P. T.; Vainiotalo, P.; Tunik, S. P.; Haukka, M.; Pakkanen, T. A. *Inorg. Chem.* **2009**, *48*, 2094.

(16) Koshevoy, I. O.; Lin, Y. C.; Karttunen, A. J.; Haukka, M.; Chou, P. T.; Tunik, S. P.; Pakkanen, T. A. *Chem. Commun.* **2009**, *27*, 2860.

(17) (a) Albota, M. A.; Xu, C.; Webb, W. W. *Appl. Opt.* **1998**, *37*, 7352. (b) Xu, C.; Webb, W. W. *J. Opt. Soc. Am. B* **1996**, *13*, 481.

(18) (a) Huang, P. H.; Shen, J. Y.; Pu, S. C.; Wen, Y. S.; Lin, J. T.; Chou, P. T.; Yeh, M. C. P. *J. Mater. Chem.* **2006**, *16*, 850. (b) Chou, C. F.; Huang, T. H.; Lin, J. T.; Hsieh, C. C.; Lai, C. H.; Chou, P. T.; Tsai, C. *Tetrahedron* **2006**, *62*, 8467.

(19) Fisher, W. G.; Wachter, E. A.; Lytle, F. E.; Armas, M.; Seaton, C. *Appl. Spectrosc.* **1998**, *52*, 536.

(20) (a) Sheik-Bahae, M.; Said, A. A.; Wei, T.-H.; Hagan, D. J.; Van Stryland, E. W. *IEEE J. Quantum Electron.* **1990**, *26*, 760. (b) Wei, T. H.; Hagan, D. J.; Sense, M. J.; Van Stryland, E. W.; Perry, J. W.; Coulter, D. R. *Appl. Phys. B: Laser Opt.* **1992**, *54*, 46. (c) Swiatkiewicz, J.; Prasad, P. N.; Reinhardt, B. A. *Opt. Commun.* **1998**, *157*, 135.

(21) (a) Drobizhev, M.; Stepanenko, Y.; Dzenis, Y.; Karotki, A.; Rebane, A.; Taylor, P. N.; Anderson, H. L. *J. Am. Chem. Soc.* **2004**, *126*, 15352. (b) Drobizhev, M.; Stepanenko, Y.; Dzenis, Y.; Karotki, A.; Rebane, A.; Taylor, P. N.; Anderson, H. L. *J. Phys. Chem. B* **2005**, *109*, 7223.

(22) Yam, V. W.-W.; Choi, S. W.-K.; Cheung, K.-K. *Organometallics* **1996**, *15*, 1734.

JP9040452